

---

# CodeGEMM: A Codebook-Centric Approach to Efficient GEMM in Quantized LLMs

---

**Gunho Park, Jeongin Bae, Byeongwook Kim, Baeseong park, Jiwon Ryu,  
Hoseung Kim, Se Jung Kwon, Dongsoo Lee**

NAVER Cloud  
[gunho.park3@navercorp.com](mailto:gunho.park3@navercorp.com)  
[github.com/naver-aics/codgemm](https://github.com/naver-aics/codgemm)

## Abstract

Weight-only quantization is widely used to mitigate the memory-bound nature of LLM inference. Codebook-based methods extend this trend by achieving strong accuracy in the extremely low-bit regime (e.g., 2-bit). However, current kernels rely on dequantization, which repeatedly fetches centroids and reconstructs weights, incurring substantial latency and cache pressure. We present *CodeGEMM*, a codebook-centric GEMM kernel that replaces dequantization with precomputed inner products between centroids and activations stored in a lightweight *Psum-book*. At inference, code indices directly gather these partial sums, eliminating per-element lookups and reducing the on-chip footprint. The kernel supports the systematic exploration of latency–memory–accuracy trade-offs under a unified implementation. On Llama-3 models, *CodeGEMM* delivers  $1.83 \times$  (8B) and  $8.93 \times$  (70B) speedups in the 2-bit configuration compared to state-of-the-art codebook-based quantization at comparable accuracy and further improves computing efficiency and memory subsystem utilization.

## 1 Introduction

Driven by the power-law scaling principle, large language models (LLMs) have grown increasingly larger, delivering remarkable advancements in performance [9, 10]. Notably, open-source models like Llama-3 [4] have reached a scale of 405 billion parameters, demonstrating significant improvements over their predecessors. However, deploying such massive models efficiently in production environments poses substantial challenges. For instance, the 405B model requires approximately 810GB of storage for its parameters alone, exceeding the memory capacity of a single multi-GPU node configured with 8 NVIDIA H100s, which offers a total of 640GB of memory. To address these limitations, extensive research has been dedicated to developing various model compression techniques aimed at reducing model size while minimizing performance degradation [8, 24, 22].

Among compression strategies, quantization has emerged as a particularly effective tool for cutting model size and bandwidth demands with minimal accuracy loss. In large language models (LLMs), challenges with activation quantization—caused by activation outliers—and the significant memory footprint of weight parameters have spurred research into weight-only quantization [6]. These methods focus on quantizing model weights to maximize memory efficiency without compromising performance.

State-of-the-art techniques show that 4-bit weight-only quantization achieves nearly the same performance as unquantized models [13, 12], with notable progress even in 3-bit quantization [21, 1]. However, in extreme low-bit (e.g., 2-bit) settings, uniform quantization suffers from significant performance degradation due to its limited representational capacity. Structured non-uniform methods

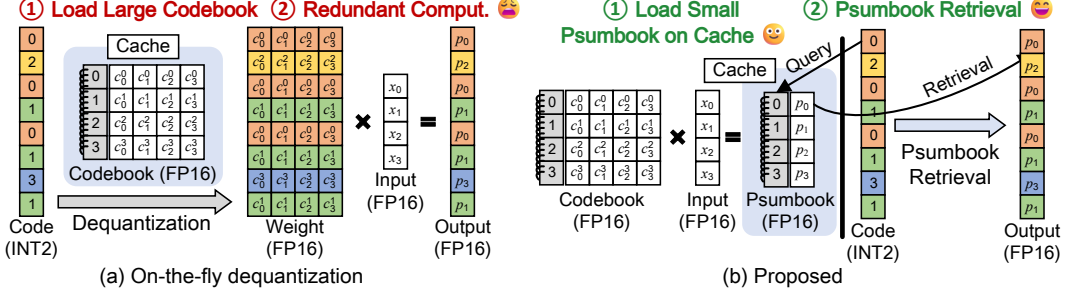


Figure 1: Comparison of matrix multiplication kernels for codebook-based quantized models. The dequantization-based kernel performs on-the-fly dequantization, requiring the entire codebook to be loaded into cache. In contrast, CodeGEMM precomputes partial sums and stores them in a Psumbook, eliminating dequantization overhead and redundant computation.

like Binary-Coded Quantization (BCQ) [30] improve performance over uniform quantization but still fall short of satisfactory results. These challenges emphasize the need for advanced non-uniform quantization techniques capable of maintaining high accuracy in extremely low-bit scenarios.

Codebook-based quantization has emerged as a promising algorithm capable of delivering superior performance in extremely low-bit environments [14, 16, 25, 26, 27]. Unlike traditional quantization methods that represent individual values with fewer bits, codebook-based quantization aims to represent data more efficiently by mapping input vectors to a limited set of centroid vectors. As a result, the original vectors are compressed and stored as codes pointing to the corresponding centroids in the codebook. However, this approach introduces a unique challenge: the efficient management of the codebook. As illustrated in Figure 1(a), unlike uniform quantization, codebook-based quantization relies on the codebook to reconstruct quantized values during computation. Without efficient codebook handling, the overhead associated with dequantization can negate the memory benefits of codebook-based quantization, potentially reducing overall efficiency.

In this paper, we propose *CodeGEMM*, a GEMM method designed to efficiently support codebook-based quantization, enabling practical speedups from extremely low-bit quantization. Unlike existing dequantization-based GEMM kernels, which load the entire codebook into programmable cache memory and rely on dequantization during computation, the proposed kernel precomputes all possible partial sum (Psum) results between the centroid and input data, storing these results as a Psumbook in cache memory (Figure 1(b)). This approach eliminates the necessity for the traditional dequantization step, during which particular centroids are retrieved from the codebook through codes. Instead, the kernel directly retrieves precomputed Psums, reducing redundant computation and significantly decreasing the space complexity required for cache storage. Moreover, the proposed kernel supports a wide range of hyperparameters that define the configuration of codebook-based quantization, facilitating the execution of various quantized models within a unified kernel. This flexibility enables users to explore and evaluate trade-offs among latency, memory usage, and accuracy, providing a versatile and efficient solution for quantized operations.

The contributions of this work are as follows:

1. We introduce *CodeGEMM*, a new approach centered on codebooks to enhance the efficiency of GEMM in codebook-based quantized LLMs. *CodeGEMM* overcomes the drawbacks of existing methods, which require loading the entire codebook into programmable cache memory for dequantization-based operations and suffer from redundant computations.
2. *CodeGEMM* accommodates a broad spectrum of codebook hyperparameters, such as the number of codebooks, vector length, and group size, all within one kernel. This adaptability allows for investigating the trade-offs between latency, memory consumption, and accuracy in codebook-based quantized models, facilitating better optimization for various use cases.
3. On Llama-3.1 models, *CodeGEMM* delivers 1.83 $\times$  (8B) and 8.93 $\times$  (70B) speedups in the 2-bit configuration compared to state-of-the-art codebook-based quantization at comparable accuracy, and further improves computing efficiency and memory subsystem utilization.

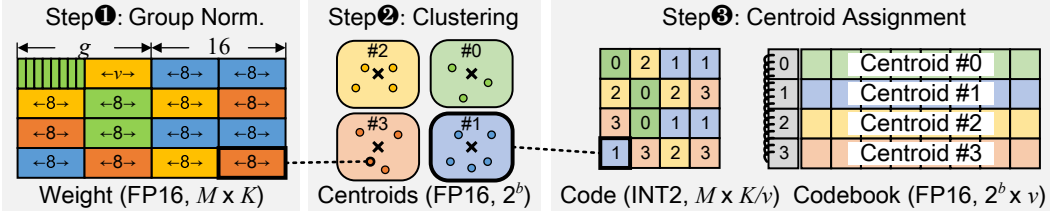


Figure 2: Illustration of quantization process of a  $(4 \times 32)$  weight matrix with  $b = 2$ ,  $m = 1$ ,  $v = 8$  and  $g = 16$ .

## 2 Background

### 2.1 Weight-only quantization

As generative language models grow larger and demand greater memory, model quantization has become essential for reducing memory footprints, minimizing model size, and improving inference efficiency. Quantization is commonly applied in two ways: (1) quantizing only the weights or (2) quantizing both weights and activations. However, activation quantization poses significant challenges due to the dynamic range of activation values and extreme outliers, termed *massive activations* [23], which exceed typical values by over  $2000\times$ .

To address these challenges, many studies have focused on weight-only quantization. GPTQ [6] uses approximate second-order information to compress weights to 4 bits with minimal accuracy loss. AWQ [13] scales salient weights based on activation magnitude to reduce quantization-induced errors. Weight-only quantization enables compact model compression, reducing memory and accelerating inference with specialized kernels [6, 13, 20, 11]. However, at extremely low precision, it still suffers notable accuracy degradation. For instance, QuIP [3] uses random rotation matrices to mitigate this issue, achieving acceptable accuracy but still facing challenges at extremely low-bit levels. To overcome these limitations, non-uniform quantization methods have been introduced [5, 25, 14, 27]. Unlike traditional uniform quantization, non-uniform approaches offer greater flexibility in representing a wider range of values, enhancing accuracy in extremely low-bit quantization scenarios [5].

### 2.2 Codebook-based quantization

Extensive research has been conducted to utilize codebook-based quantization for compressing large language models, utilizing its non-uniform properties and flexibility in representing a wide range of values [5, 16, 25, 26, 27]. In particular, GPTVQ [27] extended the GPTQ framework to incorporate codebook-based quantization, interleaving the quantization of one or more columns with updates to the remaining unquantized weights. Similarly, AQLM [5] introduced an adaptation of multi-codebook quantization for large language models, proposing a method to optimize the codebook using a calibration dataset. QuIP# [25] adopts a smoothening approach similarly to QuIP [3], applying a rotation matrix to transform weights into a space that minimizes worst-case quantization error before mapping them to structured lattice codebooks. Similarly, QTIP [26] builds on this idea by combining rotation-based smoothening with trellis-coded quantization to further enhance performance.

In this work, we build upon the additive codebook quantization strategy adopted in AQLM [5], which represents weights as the sum of multiple centroid vectors. Compared to smoothening-based approaches that rely on matrix transformations such as rotations, additive codebook quantization offers a more intuitive and inference-efficient alternative by avoiding transformation overhead during runtime. This formulation enables fast lookup-based inference and supports flexible trade-offs between accuracy, memory footprint, and latency through careful control of hyperparameters such as the number of codebooks and vector length.

Codebook-based quantization reduces memory footprint by representing the original weights as a set of vectors and approximating each individual vector with a corresponding centroid vector. As illustrated in Figure 2, a weight matrix of size  $(M \times K)$  is quantized into codebooks and corresponding codes using several key hyperparameters, including the vector length ( $v$ ), group size ( $g$ ), the number of bits per code ( $b$ ), and the number of codebooks ( $m$ ). In the first step, the parameter  $v$  specifies

the granularity at which the  $(M \times K)$  weight matrix is partitioned into vectors. Each vector is then normalized by a scaling factor to facilitate efficient clustering of weight vectors (Step ①). The normalization group size  $g$ , which is always greater than or equal to  $v$ , defines the range over which normalization is performed, ensuring consistent scaling across all vector elements. Specifically, given that the length of each vector is  $v$ , a total of  $g/v$  weight vectors are treated as a single group for normalization purposes.

After normalization, vectors are clustered and mapped to centroid values, which serve as representative values for each cluster (Step ②). A widely used approach for determining these centroid vectors is the K-means clustering algorithm, which partitions the data into a predefined number of clusters [5, 27, 14]. The algorithm iteratively initializes cluster centroids and assigns each data point to the nearest cluster based on a chosen distance metric, repeating this process until convergence is achieved.

Each centroid vector is assigned a unique index, referred to as a code. The number of clusters is set to  $2^b$ , where  $b$  denotes the number of bits per code, allowing representation of values ranging from 0 to  $2^b - 1$ . A codebook that maps each code to its corresponding centroid vector is constructed (Step ③), and original weight values can subsequently be reconstructed by decoding the codes using this codebook. To minimize quantization error, multi-codebook concept has been proposed [5, 2], which performs the quantization process  $m$  times, constructing  $m$  codebooks and summing their values to represent the original weight value more accurately.

Since applying codebook-based quantization makes  $v$  sized full-precision values to be represented by  $m$  different codes of  $b$  bit precision, the average bit per weight is decided by these hyperparameters. Specifically, the number of bits per weight is calculated by dividing the total quantized bits by the number of weights. The total bit size, and consequently, the average bit per weight  $\bar{q}$ , can be expressed as follows:

$$\begin{aligned} \bar{q} &= \frac{S_{\text{codebook}} + S_{\text{code}} + S_{\text{norm}}}{M \cdot K} \\ &= \frac{16 \cdot m \cdot 2^b \cdot v + b \cdot m \cdot M \cdot \frac{K}{v} + 16 \cdot M \cdot \frac{K}{g}}{M \cdot K}, \end{aligned} \quad (1)$$

where the precision of each vector element in the codebook is set to FP16. Equation 1 also reveals that multiple combinations of hyperparameters can achieve the same average bit per weight. For example, as shown in Table 1, various combinations including  $(v, m, b, g) = (4, 1, 8, -1)$  and  $(v, m, b, g) = (16, 3, 8, 32)$  result in almost the same average bit per weight of 2. Since our goal is to maintain model accuracy under extremely low-bit quantization, achieving an optimal trade-off between bit precision and accuracy is essential. However, the impact of these hyperparameters on model accuracy and inference latency remains largely unexplored, necessitating extensive investigation through comprehensive experimental studies. In this paper, we analyze how different hyperparameter combinations with similar average bits per weight influence the trade-offs between memory footprint and performance, providing valuable insights into optimizing quantized models.

Table 1: Average bits per weight for various quantization configurations.  $q_{\text{code}}$ ,  $q_{\text{codebook}}$ , and  $q_{\text{norm}}$  represent the average bits allocated to codes, codebooks, and group normalization factors, respectively. A value of  $g = -1$  indicates row-wise group normalization.

v	m	b	g	$q_{\text{code}}$	$q_{\text{codebook}}$	$q_{\text{norm}}$	$\bar{q}$
4	1	8	-1	2.0	0.001	0.004	2.005
8	2	8	-1	2.0	0.004	0.004	2.008
16	4	8	-1	2.0	0.016	0.004	2.020
8	1	8	16	1.0	0.002	1.000	2.002
16	3	8	32	1.5	0.012	0.500	2.012

### 2.3 Kernels for Quantized LLM

Recent weight-only quantization techniques, aimed at reducing bit-widths to sub-4-bit levels to enhance memory efficiency, are also focused on achieving practical speedups. For instance, GPTQ [6] and AWQ [13] provide INT3-FP and INT4-FP kernels for uniform quantization, respectively, alongside their quantization methodologies. While these kernels achieve reduced latency relative to the

FP16 cuBLAS baseline, they fall short of improving computational efficiency. This limitation arises as the benefits primarily stem from more efficient data movement facilitated by quantization, rather than from the computational performance itself. To address this issue, LUT-GEMM [20] introduces a kernel that reduces computational complexity by utilizing a lookup table, leveraging the BCQ format to represent quantized weights.

Especially in codebook-based quantization, the current kernel [5] relies on a dequantization process. This process reconstructs the original weights by using the codes to retrieve the corresponding centroids from the codebook. These codes serve as indices for querying the codebook, where the corresponding centroids are retrieved and used as dequantized weights. The  $(M \times K/v)$  code matrix retrieves centroid vectors of length  $v$ , reconstructing a dequantized matrix of the same shape as the original matrix  $(M \times K)$ . Subsequent matrix multiplication with the input matrix is then performed in the same manner as with the original weight matrix. To support efficient dequantization, current kernels load the entire codebook in programmable cache to enable rapid retrieval of centroid vectors. However, this approach leads to significant memory write overhead during the codebook load phase. Furthermore, as the codebook size increases, loading the entire codebook in programmable cache becomes more challenging. For instance, in the AQLM  $(1 \times 16)$  kernel the codebook requires  $2^{16}$  centroids of length  $v = 8$ , each represented in FP16. This requires  $2^{16} \times 1 \times 8 \times 2$  bytes ( $=1\text{MB}$ ) of shared memory, far exceeding the capacity of both A100 (164KB) and H100 (224KB). As a result, the codebook cannot reside in shared memory and must be repeatedly fetched from DRAM, significantly increasing latency. Furthermore, while this dequantization approach effectively optimizes data movement, it does not reduce computational complexity, which remains identical to that of the original matrix multiplication.

### 3 CodeGEMM: Codebook-based GEMM

**Motivation.** Figure 1 illustrates the matrix multiplication process in codebook-based quantization and highlights two key challenges. First, loading the entire codebook into programmable cache incurs substantial overhead that scales with the size of the codebook and is repeated by each thread block, leading to performance degradation in large-scale deployments. Second, computations are often redundant, as each input vector interacts with a limited set of centroids, resulting in repeated calculations across the output matrix. To address these challenges, we propose a method that minimizes codebook load overhead and avoids redundant computation, enabling more efficient use of limited on-chip cache and improving overall efficiency.

**Methodology.** *CodeGEMM* introduces a codebook-centric approach to efficient matrix multiplication in quantized LLMs. Instead of loading the entire codebook, *CodeGEMM* stores precomputed results of the inner products between the centroid vectors and input activations in the programmable cache. This approach reduces space complexity and eliminates the need for dequantization operations that retrieve centroids for each code from the codebook. Instead, the kernel repeatedly utilizes the precomputed results, significantly reducing the computational complexity.

Figure 3 illustrates the computation process of CodeGEMM, depicting a matrix multiplication operation between a weight tile of dimensions  $(t_h \times t_w)$  and an input tile of dimensions  $(t_w \times 1)$ . Initially, the input tile is partitioned into inputs of dimensions  $(t_w/v \times v \times 1)$  to facilitate efficient computation with centroids stored in the codebook (Step ①). These segmented inputs are represented as  $x_k^j = x_{v \times j+k}$ , where  $j \in [0, 1, \dots, t_w/v - 1]$  and  $k \in [0, 1, \dots, v - 1]$ . The corresponding code matrix is similarly partitioned into code tiles of dimensions  $(t_h \times t_w/v)$  to align with the input tiles for effective computation. In our implementation, we set  $t_w = 32$  and  $t_h = 2048$  to align with hardware-friendly tiling strategies and to maximize reuse of the Psumbook within each thread block. Next, each segmented input computes inner products with the centroids to generate partial sums (Psums), which are then stored as a Psumbook in the programmable cache (Step ②). Each entry in the Psumbook,  $p_i^j$ , is calculated as follows:

$$p_i^j = \sum_{k=0}^{v-1} c_k^i \times x_k^j, \quad i \in [0, 1, \dots, 2^b - 1] \quad (2)$$

By storing the Psumbook in the programmable cache instead of the full codebook, *CodeGEMM* replaces the conventional process of fetching and computing with centroids for each code with a more

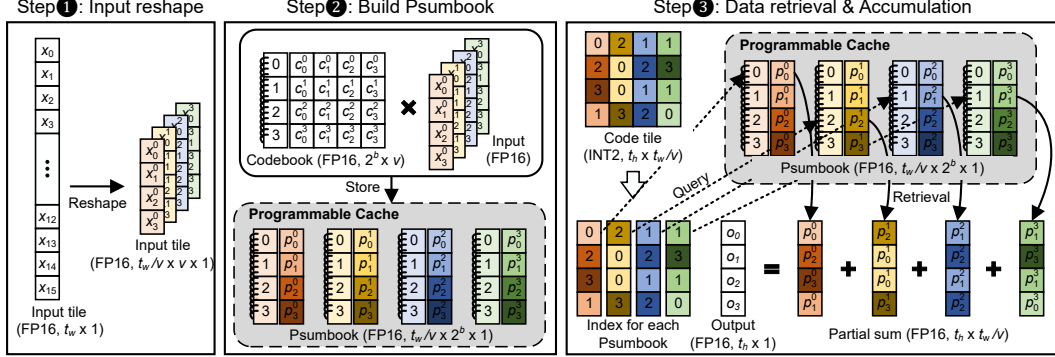


Figure 3: Overview of the *CodeGEMM* kernel operation for codebook-based quantized models. 1) Input data is reshaped into vectors to align with the codebook dimensions. 2) Precomputed inner products between the codebook and input vectors are stored in the Psumbook within the programmable cache, significantly reducing computational overhead. 3) During computation, codes query the corresponding partial sums from the Psumbook, which are then accumulated to generate the output efficiently without requiring on-the-fly dequantization.

efficient retrieval of precomputed Psoms using code as a key. This not only reduces computational complexity but also lowers space complexity, as only the scalar inner product results are cached rather than the full centroid vectors. Finally, the partial sums corresponding to each input are retrieved from the Psumbook via code-based indexing and then accumulated to generate the final output activations for the thread block (Step 3). In contrast to existing kernels that load the entire codebook into the programmable cache, our approach of storing precomputed inner product results allows for significantly more efficient computations for codebook-based quantized LLMs.

**Computational complexity.** In a matrix multiplication operation with a weight matrix of size  $(M \times K)$  and an input matrix of size  $(K \times N)$ , the computational complexity of a standard GEMM kernel is given as  $\mathcal{O}(MNK)$ . This complexity also applies to dequantization-based kernels, as they improve data movement efficiency through quantization but do not reduce the overall computation cost.

In contrast, *CodeGEMM* reduces the computational workload by precomputing all inner product results between the centroid vectors and input activations, storing them in a Psumbook, and replacing repeated computations with simple retrieval operations. This allows *CodeGEMM* to achieve a lower computational complexity compared to conventional methods. The computational complexity of *CodeGEMM*, assuming  $M \gg 2^b$ , is expressed as follows:

$$\begin{aligned} C &= C_{build} + C_{read} = \mathcal{O}\left(m \cdot 2^b \cdot v \cdot \frac{K}{v} \cdot N\right) + \mathcal{O}\left(m \cdot M \cdot \frac{K}{v} \cdot N\right) \\ &= \mathcal{O}\left(mMNK \left(\frac{2^b}{M} + \frac{1}{v}\right)\right) \approx \mathcal{O}\left(MNK \cdot \frac{m}{v}\right), \end{aligned} \quad (3)$$

where  $C_{build}$  and  $C_{read}$  represent the computational complexity of building the Psumbook and retrieving values from it, respectively. Consequently, *CodeGEMM* achieves a computational reduction factor of  $(m/v)$  compared to conventional kernels, where  $m$  is the number of codebooks and  $v$  is the vector length—both crucial for optimizing performance. This enables *CodeGEMM* to enhance data movement efficiency through quantization, like traditional dequantization-based kernels, while also reducing computational complexity for higher efficiency.

**Space Complexity.** Dequantization-based GEMM kernels load the entire codebook into the programmable cache to perform computations. In this case, the space complexity is given by  $\mathcal{O}(m \cdot 2^b \cdot v)$ , which corresponds to the full size of the codebook. In contrast, the space complexity of *CodeGEMM* is  $\mathcal{O}(m \cdot 2^b \cdot t_w/v)$ , where  $t_w$  denotes the width of the weight tile. Since *CodeGEMM* stores precomputed inner product results rather than full centroid vectors, its space complexity is inversely proportional to the vector length  $v$ , resulting in a smaller cache footprint. This reduction in memory

requirements allows *CodeGEMM* to achieve more efficient cache utilization, making it better suited for accelerators with limited programmable cache sizes.

## 4 Experiments

**Setup.** We evaluate *CodeGEMM* by exploring the trade-offs across key hyperparameters, focusing on three primary metrics relevant to LLM compression: memory footprint, latency, and accuracy. The memory footprint is quantified using the average number of bits per weight  $\bar{q}$  and computed according to Equation 1. Latency is measured to compare raw kernel performance for matrix multiplication, assuming the shape of linear layers used in Llama-3 [4], a widely adopted architecture. Specifically, latency is reported as the sum of kernel execution times for all linear layers in a single Transformer decoder block without layer fusion. All latency measurements are performed on an NVIDIA A100 80GB GPU. Throughput (or, equivalently, end-to-end latency) is additionally measured using the Llama implementation provided by the HuggingFace [29] library with layer fusion. Although this library is not optimized for high-throughput inference, it remains one of the most widely used frameworks and thus serves as a practical baseline. Accuracy is evaluated using the lm-eval-harness [7] benchmark suite across both zero-shot and 5-shot settings on standard tasks.

**Memory Footprint vs. Latency.** Table 2 presents the kernel-level latency of various quantized matrix multiplication methods on 2-bit quantized Llama3 models (8B and 70B). LUTGEMM [20], designed for uniform quantization, achieves strong performance by eliminating redundant computations through efficient use of lookup tables. QuIP# [25] and QTIP [26], which rely on smoothing-based transformations, mitigate the associated overhead through highly optimized fused kernels, demonstrating competitive latency. AQLM [5] with the  $2 \times 8$  configuration improves data movement efficiency via quantization, resulting in moderate latency reduction despite retaining the same computational complexity as the FP16 baseline. However, AQLM-1  $\times$  16 suffers from significantly higher latency due to inefficient dequantization caused by its large codebook (e.g.,  $2^{16}$  entries), which exceeds on-chip cache capacity. In contrast, *CodeGEMM* achieves up to  $2.18 \times$  and  $1.64 \times$  speed-ups over the FP16 baseline and AQLM, respectively, at the same average bit precision. This improvement is due to both the use of precomputed inner products, which reduce computational complexity, and the efficient utilization of shared memory.

Figure 4(a) shows the relationship between memory footprint and latency of the Llama-3.1-8B model under a single batch operation. As shown in Table 1, codebook-based quantization enables diverse configurations within a given memory footprint by adjusting hyperparameter settings. According to Equation 1, the group size  $g$  impacts the memory footprint. Smaller group sizes increase the total memory footprint, leading to higher latency in memory-bound operations. For  $g \geq 32$ , the fine-grained group normalization incurs minimal latency overhead despite the growing memory footprint. However, as  $g$  decreases further, the overhead becomes more pronounced, particularly in per-vector normalization (i.e.,  $g = v$ ), where the latency rises sharply. Additionally, this overhead is amplified when the group normalization scale factor constitutes a larger proportion of the total memory footprint, which is more likely when the number of codebooks  $m$  is small.

Table 2: Kernel-level latency ( $\mu$ s) of quantized matrix multiplication in 2-bit quantized Llama3 models (8B and 70B). *CodeGEMM* achieves consistently lower latency than other methods.

	cuBLAS (fp16)	LUTGEMM (q2-g128)	QuIP# (e8p)	QTIP (r2)	AQLM (1x16)	AQLM (2x8)	CodeGEMM (m2v8g128)	CodeGEMM (m1v4g128)
8B	332.45	160.1	162.63	189.94	645.51	250.12	172.18	<b>152.69</b>
70B	1111.36	299.9	403.59	477.04	2285.5	674.67	373.49	<b>293.82</b>

**Efficiency and Utilization.** We measured DRAM traffic proxies and power efficiency using nvidia-smi [18] telemetry. Metrics were sampled at a 100 ms cadence over a 10 s window and averaged across trials. Memory utilization represents the fraction of the sampling interval during which device (global) memory was actively read from or written to [18]. As summarized in Table 3, on a matrix multiplication workload with  $M=1$ ,  $N=28672$ , and  $K=8192$ , *CodeGEMM* delivers substantially higher compute efficiency (GFLOPS/W) than dequantization-based kernels. Parenthetical values denote two-sigma error margins over 128 samples. Beyond lower latency, *CodeGEMM* also

shows higher energy efficiency and improved memory-subsystem utilization, indicating reduced and more structured DRAM access relative to dequantization-based approaches.

Table 3: Kernel-level Performance evaluation on a GEMV with  $(M, N, K) = (1, 28672, 8192)$ . Performance metrics are obtained from `nvidia-smi` telemetry. *CodeGEMM* delivers higher power efficiency and improved memory utilization than dequantization-based codebook kernels.

Method	TFLOPS	Power (W)	GFLOPS/W	GPU Util (%)	Mem Util (%)
cUBLAS	1.58	318.55 ( $\pm 6.26$ )	4.95	96.87 ( $\pm 0.73$ )	96.94 ( $\pm 0.48$ )
AQLM-1x16	0.75	126.54 ( $\pm 0.49$ )	5.93	99.00 ( $\pm 0.00$ )	6.00 ( $\pm 0.00$ )
AQLM-2x8	2.59	254.20 ( $\pm 2.47$ )	10.18	92.84 ( $\pm 1.58$ )	19.96 ( $\pm 0.39$ )
CodeGEMM-m2v8g128	5.43	304.69 ( $\pm 6.11$ )	17.83	85.32 ( $\pm 1.58$ )	43.75 ( $\pm 0.95$ )
CodeGEMM-m1v4g128	6.12	316.38 ( $\pm 8.37$ )	<b>19.36</b>	84.47 ( $\pm 2.28$ )	49.80 ( $\pm 1.21$ )

**Memory Footprint vs. Accuracy.** Figure 4(b) shows the relationship between memory footprint and accuracy of quantized models across various hyperparameter configurations. Perplexity, measured using the WikiText-2 dataset, is used to evaluate accuracy. *CodeGEMM* builds on block-wise codebook optimization [5] and incorporates fine-grained group normalization for enhanced performance. As average bits per weight increase, models demonstrate greater representational capacity, resulting in lower perplexity. Fine-grained group normalization reduces quantization error, but it increases memory footprint as the normalization factor grows. Under row-wise group normalization ( $g = -1$ ), increasing the number of codebooks ( $m$ ) while keeping the average bit precision fixed leads to improved accuracy, as the model can better approximate the original weights with additive codebooks. However, as  $g$  becomes smaller (i.e., more fine-grained), this accuracy gain from increasing  $m$  diminishes, and models tend to exhibit similar performance for a given  $\bar{q}$ , regardless of the number of codebooks.

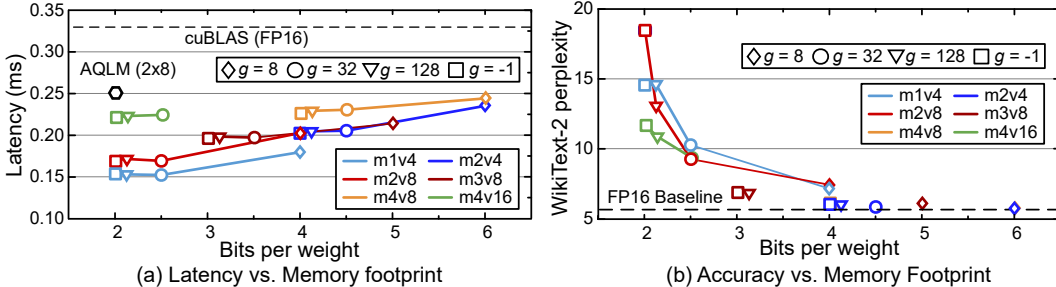


Figure 4: Latency and accuracy trade-offs for the Llama-3.1-8B model under various configurations.

**Throughput vs. Accuracy.** While many studies on quantization have focused on the trade-off between memory footprint and accuracy to achieve better performance, the relationship between throughput (or, equivalently, decode-phase latency) and accuracy has often been overlooked. However, in real-world applications and service-level deployments, latency is often a critical constraint that directly impacts user experience and system efficiency.

Table 4 compares the accuracy of *CodeGEMM* against both uniform and codebook-based quantization methods. We include FlexRound [12] as a representative uniform quantization baseline and AQLM [5] for codebook-based quantization. To further improve accuracy, we also apply PV-Tuning [16], a recently proposed post-quantization calibration method for codebook-based models. Figure 5 reports the resulting accuracy–throughput trade-offs. Throughput for FlexRound is measured using LUT-GEMM [20], a state-of-the-art kernel optimized for uniformly quantized models. While FlexRound demonstrates strong throughput at 2-bit precision, it suffers from the worst accuracy among all methods, highlighting the limitations of uniform quantization in extremely low-bit settings. The recent vector-quantization approach VPTQ [14] achieves an average accuracy of 57.98, slightly higher than *CodeGEMM* without PV-Tuning. However, its kernel is implemented as a straightforward dequantize-then-multiply pipeline without operator fusion, which introduces dequantization overhead and leads to lower throughput than FP16.

AQLM, with its dequantization-based kernel, achieves notably higher accuracy in such settings but exhibits poor throughput due to the overhead of repeatedly loading large codebooks. Specifically, AQLM ( $1 \times 16$ ) achieves the best accuracy under a 2-bit memory budget by using a large codebook ( $b = 16$ ), but this configuration exceeds the capacity of the programmable cache. As a result, it incurs inefficient memory access and dequantization latency, leading to a suboptimal throughput–accuracy trade-off. AQLM ( $2 \times 8$ ) improves throughput over the FP16 baseline, but only marginally, because it still pays the dequantization cost and maintains similar computational complexity. In contrast, *CodeGEMM* delivers significantly better throughput while maintaining competitive accuracy. Moreover, it shows strong synergy with PV-Tuning, achieving results comparable to or better than AQLM with less computational overhead. Between different *CodeGEMM* configurations, the  $m1v4$  variant consistently outperforms  $m2v8$  in both throughput and accuracy, even though both configurations maintain a similar average bit precision. This aligns with the kernel-level latency trend observed in Figure 4(a), while diverging slightly from the perplexity trend in Figure 4(b), suggesting that end-to-end throughput–accuracy behavior can differ from perplexity metrics. Overall, *CodeGEMM* achieves a  $1.83 \times$  end-to-end speedup over dequantization-based kernels at comparable accuracy (Figure 5(a)).

Table 4: Accuracy of various quantization methods on the Llama-3.1-8B-Instruct model. The Average column represents the mean accuracy across all tasks, including MMLU (5-shot) and 0-shot tasks such as WinoGrande (WG), HellaSwag (HS), ARC-Easy (ARC-E), and ARC-Challenge (ARC-C).

Method	$\bar{q}$	tok/s	MMLU	WG	HS	ARC-E	ARC-C	Avg.
FP16	16.000	103.8	68.39	73.95	79.2	79.63	55.03	71.26
FlexRound-q2g128 [12]	2.125	205.3	24.27	55.16	43.78	24.75	24.57	41.65
AQLM-2x8 [5]	2.005	124.5	42.29	58.25	61.40	46.25	30.89	47.82
+PV-Tuning	2.005	124.5	55.13	69.14	72.43	71.25	45.73	62.74
AQLM-1x16 [5]	2.213	49.0	58.74	68.75	70.21	73.99	46.16	63.57
+PV-Tuning	2.213	49.0	<b>60.72</b>	<b>70.24</b>	<b>74.33</b>	<b>74.92</b>	<b>48.89</b>	<b>65.82</b>
<b>CodeGEMM-m1v4g128</b>	2.126	<b>228.3</b>	45.16	58.96	63.07	63.97	38.48	53.93
+PV-Tuning	2.126	<b>228.3</b>	57.42	69.06	73.85	73.15	46.33	63.96
<b>CodeGEMM-m2v8g128</b>	2.127	214.4	42.83	60.54	62.84	60.14	37.03	52.67
+PV-Tuning	2.127	214.4	55.42	68.75	73.02	73.91	47.70	63.76

**Scaling to Larger Models.** To evaluate the scalability of *CodeGEMM* for larger language models, we assess its performance on the Llama-3.1-70B model under various quantization configurations. Table 5 compares *CodeGEMM* with uniform quantization methods such as GPTQ [6] and FlexRound [12], as well as the codebook-based method AQLM. As model size increases from 8B to 70B, latency improvements relative to the AQLM become more pronounced. While the overall performance trends are consistent with those observed in the 8B model, we observe that ( $1 \times 16$ ) suffers from significantly degraded throughput at 70B due to the large codebook size (e.g.,  $2^{16}$  entries), which exceeds shared memory limits and introduces excessive dequantization overhead. In contrast, *CodeGEMM* achieves a favorable trade-off by leveraging fine-grained group normalization to improve accuracy with minimal increases in memory footprint and latency. The benefit of fine-grained normalization is evident in the widening accuracy gap between *CodeGEMM* and AQLM ( $2 \times 8$ ), which uses row-wise normalization, at 70B relative to 8B. Consequently, *CodeGEMM* matches the accuracy of AQLM ( $1 \times 16$ ) while delivering an  $8.93 \times$  throughput advantage (Figure 5(b)). These results demonstrate that *CodeGEMM* scales effectively to large models while maintaining competitive performance.

## 5 Related Work

**Look-Up Table-Based Computation.** Several prior works have leveraged look-up tables (LUTs) to improve computational efficiency, both at the kernel level [20, 15] and in specialized hardware designs [28, 17, 19]. However, these approaches primarily support uniform or binary-coded quantization formats, and do not extend to codebook-based non-uniform quantization. In contrast, *CodeGEMM* is designed to naturally support codebook-based quantization while also being generalizable to uniform and binary formats through appropriate codebook configurations. Specifically, uniform and binary quantization can be accommodated by defining centroids as  $c \in \{0, 1\}^v$  for uniform quantization and

Table 5: Accuracy of various quantization methods on the Llama-3.1-70B model.

Method	$\bar{q}$	tok/s	MMLU	WG	HS	ARC-E	ARC-C	Avg.
FP16	16.000	<b>OOM</b>	78.58	79.64	85.03	86.66	64.93	78.97
GPTQ-q2g128	2.125	41.7	26.35	53.04	49.04	48.95	29.52	41.38
FlexRound-q2g128	2.125	41.7	26.70	53.59	50.67	25.13	24.83	36.58
AQLM-2x8	2.002	19.0	61.45	59.59	52.83	48.82	28.67	50.27
AQLM-1x16	2.055	5.5	<b>73.07</b>	<b>76.16</b>	<b>80.83</b>	<b>82.20</b>	<b>57.17</b>	<b>73.89</b>
<b>CodeGEMM-m1v4g128</b>	2.125	<b>51.2</b>	68.15	74.90	75.37	79.42	52.73	70.11
<b>CodeGEMM-m1v4g32</b>	2.500	49.1	71.21	76.64	79.43	82.41	56.06	73.15

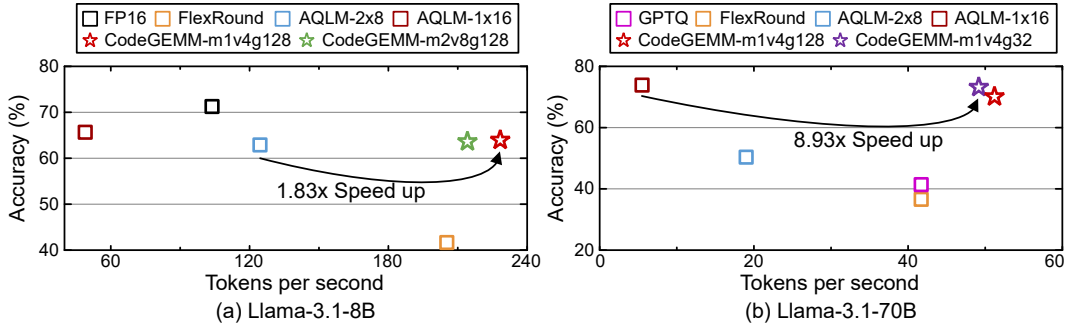


Figure 5: Latency and accuracy trade-offs for the Llama-3.1-8B model under various configurations.

$c \in \{-1, 1\}^v$  for binary quantization. This generality makes *CodeGEMM* particularly suitable for deployment as a fixed-function ASIC kernel, as it enables support for diverse quantization formats under a unified hardware architecture.

**Codebook-based Quantization.** Beyond additive codebooks, recent work has explored highly structured designs that integrate a rotation with the codebook itself. QuIP# [25] and QTIP [26] both pair their lattice- and trellis-coded codebooks with an inference-time *smoothening* rotation, and each work supplies a carefully hand-tuned kernel that fuses the rotation with subsequent look-ups. In contrast, the additive codebooks we target require only a lightweight table lookup and accumulation without rotation, so dequantization remains simple and fast. This design lets *CodeGEMM* deliver competitive 2-bit accuracy while retaining a single, reusable kernel that scales across a broad range of quantization settings.

## 6 Conclusion

**Summary.** This paper presents *CodeGEMM*, an efficient matrix multiplication method for codebook-based quantized models. Instead of loading the full codebook into programmable cache, *CodeGEMM* precomputes and stores results in a Psumbook, reducing both space and computational complexity. Experiments show that *CodeGEMM* outperforms state-of-the-art kernels in latency while maintaining high accuracy in extremely low-bit quantization.

**Limitations.** *CodeGEMM* requires the Psumbook to reside in on-chip shared memory, which constrains the usable codebook size. Very large codebooks (e.g.,  $b=16$  with  $2^{16}$  entries) exceed current GPU cache limits. In practice, we therefore fix the per-codebook width to  $b=8$  and recover accuracy via fine-grained group normalization, which adds negligible latency and yields favorable accuracy-efficiency trade-offs under realistic hardware constraints. A second limitation is large-batch throughput: *CodeGEMM* underperforms compared to Tensor Core-based cuBLAS when the batch size is large (e.g.,  $M > 32$ ). This behavior is common to CUDA Core-based quantized GEMM kernels and reflects the current commercial GPU architecture rather than an inefficiency of the algorithm itself. Overall, while *CodeGEMM* excludes extremely large codebooks and is not optimized for large batches, its hardware-algorithm co-design addresses key inefficiencies of traditional codebook quantization, reducing both computational and space complexity.

## References

- [1] Saleh Ashkboos, Amirkeivan Mohtashami, Maximilian L Croci, Bo Li, Pashmina Cameron, Martin Jaggi, Dan Alistarh, Torsten Hoefer, and James Hensman. Quarot: Outlier-free 4-bit inference in rotated llms. *arXiv preprint arXiv:2404.00456*, 2024.
- [2] Artem Babenko and Victor Lempitsky. Additive quantization for extreme vector compression. In *Proceedings of the IEEE Conference on Computer Vision and Pattern Recognition*, pages 931–938, 2014.
- [3] Jerry Chee, Yaohui Cai, Volodymyr Kuleshov, and Christopher M De Sa. Quip: 2-bit quantization of large language models with guarantees. *Advances in Neural Information Processing Systems*, 36, 2024.
- [4] Abhimanyu Dubey, Abhinav Jauhri, Abhinav Pandey, Abhishek Kadian, Ahmad Al-Dahle, Aiesha Letman, Akhil Mathur, Alan Schelten, Amy Yang, Angela Fan, et al. The llama 3 herd of models. *arXiv preprint arXiv:2407.21783*, 2024.
- [5] Vage Egiazarian, Andrei Panferov, Denis Kuznedelev, Elias Frantar, Artem Babenko, and Dan Alistarh. Extreme compression of large language models via additive quantization. *arXiv preprint arXiv:2401.06118*, 2024.
- [6] Elias Frantar, Saleh Ashkboos, Torsten Hoefer, and Dan Alistarh. Gptq: Accurate post-training quantization for generative pre-trained transformers. *arXiv preprint arXiv:2210.17323*, 2022.
- [7] Leo Gao, Jonathan Tow, Baber Abbasi, Stella Biderman, Sid Black, Anthony DiPofi, Charles Foster, Laurence Golding, Jeffrey Hsu, Alain Le Noac'h, Haonan Li, Kyle McDonell, Niklas Muennighoff, Chris Ociepa, Jason Phang, Laria Reynolds, Hailey Schoelkopf, Aviya Skowron, Lintang Sutawika, Eric Tang, Anish Thite, Ben Wang, Kevin Wang, and Andy Zou. The language model evaluation harness, 07 2024.
- [8] Jung Hwan Heo, Jeonghoon Kim, Beomseok Kwon, Byeongwook Kim, Se Jung Kwon, and Dongsoo Lee. Rethinking channel dimensions to isolate outliers for low-bit weight quantization of large language models. *arXiv preprint arXiv:2309.15531*, 2023.
- [9] Jordan Hoffmann, Sebastian Borgeaud, Arthur Mensch, Elena Buchatskaya, Trevor Cai, Eliza Rutherford, Diego de Las Casas, Lisa Anne Hendricks, Johannes Welbl, Aidan Clark, et al. Training compute-optimal large language models. *arXiv preprint arXiv:2203.15556*, 2022.
- [10] Jared Kaplan, Sam McCandlish, Tom Henighan, Tom B Brown, Benjamin Chess, Rewon Child, Scott Gray, Alec Radford, Jeffrey Wu, and Dario Amodei. Scaling laws for neural language models. *arXiv preprint arXiv:2001.08361*, 2020.
- [11] Young Jin Kim, Rawn Henry, Raffy Fahim, and Hany Hassan Awadalla. Finequant: Unlocking efficiency with fine-grained weight-only quantization for llms. *arXiv preprint arXiv:2308.09723*, 2023.
- [12] Jung Hyun Lee, Jeonghoon Kim, Se Jung Kwon, and Dongsoo Lee. Flexround: Learnable rounding based on element-wise division for post-training quantization. In *International Conference on Machine Learning*, pages 18913–18939. PMLR, 2023.
- [13] Ji Lin, Jiaming Tang, Haotian Tang, Shang Yang, Wei-Ming Chen, Wei-Chen Wang, Guangxuan Xiao, Xingyu Dang, Chuang Gan, and Song Han. Awq: Activation-aware weight quantization for on-device llm compression and acceleration. *Proceedings of Machine Learning and Systems*, 6:87–100, 2024.
- [14] Yifei Liu, Jicheng Wen, Yang Wang, Shengyu Ye, Li Lyna Zhang, Ting Cao, Cheng Li, and Mao Yang. Vptq: Extreme low-bit vector post-training quantization for large language models. *arXiv preprint arXiv:2409.17066*, 2024.
- [15] Saeed Maleki. Look-up mai gemm: Increasing ai gemms performance by nearly 2.5 x via msgemm. *arXiv preprint arXiv:2310.06178*, 2023.

[16] Vladimir Malinovskii, Denis Mazur, Ivan Ilin, Denis Kuznedelev, Konstantin Burlachenko, Kai Yi, Dan Alistarh, and Peter Richtarik. Pv-tuning: Beyond straight-through estimation for extreme llm compression. *arXiv preprint arXiv:2405.14852*, 2024.

[17] Zhiwen Mo, Lei Wang, Jianyu Wei, Zhichen Zeng, Shijie Cao, Lingxiao Ma, Naifeng Jing, Ting Cao, Jilong Xue, Fan Yang, et al. Lut tensor core: Lookup table enables efficient low-bit llm inference acceleration. *arXiv preprint arXiv:2408.06003*, 2024.

[18] NVIDIA Corporation. Nvidia system management interface (nvidia-smi) documentation. <https://docs.nvidia.com/deploy/nvidia-smi/index.html>, 2025. Accessed: 2025-10-22.

[19] Gunho Park, Hyeokjun Kwon, Jiwoo Kim, Jeongin Bae, Baeseong Park, Dongsoo Lee, and Youngjoo Lee. Figlut: An energy-efficient accelerator design for fp-int gemm using look-up tables. In *2025 IEEE International Symposium on High Performance Computer Architecture (HPCA)*, pages 1098–1111. IEEE, 2025.

[20] Gunho Park, Baeseong Park, Minsub Kim, Sungjae Lee, Jeonghoon Kim, Beomseok Kwon, Se Jung Kwon, Byeongwook Kim, Youngjoo Lee, and Dongsoo Lee. Lut-gemm: Quantized matrix multiplication based on luts for efficient inference in large-scale generative language models. *arXiv preprint arXiv:2206.09557*, 2024.

[21] Wenqi Shao, Mengzhao Chen, Zhaoyang Zhang, Peng Xu, Lirui Zhao, Zhiqian Li, Kaipeng Zhang, Peng Gao, Yu Qiao, and Ping Luo. Omnidquant: Omnidirectionally calibrated quantization for large language models. *arXiv preprint arXiv:2308.13137*, 2023.

[22] Sharath Turuvekere Sreenivas, Saurav Muralidharan, Raviraj Joshi, Marcin Chochowski, Mostofa Patwary, Mohammad Shoeybi, Bryan Catanzaro, Jan Kautz, and Pavlo Molchanov. Llm pruning and distillation in practice: The minitron approach. *arXiv preprint arXiv:2408.11796*, 2024.

[23] Mingjie Sun, Xinlei Chen, J Zico Kolter, and Zhuang Liu. Massive activations in large language models. *arXiv preprint arXiv:2402.17762*, 2024.

[24] Mingjie Sun, Zhuang Liu, Anna Bair, and J Zico Kolter. A simple and effective pruning approach for large language models. *arXiv preprint arXiv:2306.11695*, 2023.

[25] Albert Tseng, Jerry Chee, Qingyao Sun, Volodymyr Kuleshov, and Christopher De Sa. Quip#: Even better llm quantization with hadamard incoherence and lattice codebooks. *arXiv preprint arXiv:2402.04396*, 2024.

[26] Albert Tseng, Qingyao Sun, David Hou, and Christopher M De Sa. Qtip: Quantization with trellises and incoherence processing. *Advances in Neural Information Processing Systems*, 37:59597–59620, 2024.

[27] Mart van Baalen, Andrey Kuzmin, Markus Nagel, Peter Couperus, Cedric Bastoul, Eric Mahurin, Tijmen Blankevoort, and Paul Whatmough. Gptvq: The blessing of dimensionality for llm quantization. *arXiv preprint arXiv:2402.15319*, 2024.

[28] Jianyu Wei, Shijie Cao, Ting Cao, Lingxiao Ma, Lei Wang, Yanyong Zhang, and Mao Yang. T-mac: Cpu renaissance via table lookup for low-bit llm deployment on edge. In *Proceedings of the Twentieth European Conference on Computer Systems*, pages 278–292, 2025.

[29] Thomas Wolf, Lysandre Debut, Victor Sanh, Julien Chaumond, Clement Delangue, Anthony Moi, Pierrick Cistac, Tim Rault, Rémi Louf, Morgan Funtowicz, Joe Davison, Sam Shleifer, Patrick von Platen, Clara Ma, Yacine Jernite, Julien Plu, Canwen Xu, Teven Le Scao, Sylvain Gugger, Mariama Drame, Quentin Lhoest, and Alexander M. Rush. Transformers: State-of-the-art natural language processing. In *Proceedings of the 2020 Conference on Empirical Methods in Natural Language Processing: System Demonstrations*, pages 38–45, Online, October 2020. Association for Computational Linguistics.

[30] Haoran You, Yipin Guo, Yichao Fu, Wei Zhou, Huihong Shi, Xiaofan Zhang, Souvik Kundu, Amir Yazdanbakhsh, and Yingyan Celine Lin. Shiftaddllm: Accelerating pretrained llms via post-training multiplication-less reparameterization. *arXiv preprint arXiv:2406.05981*, 2024.

## NeurIPS Paper Checklist

### 1. Claims

Question: Do the main claims made in the abstract and introduction accurately reflect the paper's contributions and scope?

Answer: [\[Yes\]](#)

Justification: We have clearly made the main claims in the abstract and introduction.

Guidelines:

- The answer NA means that the abstract and introduction do not include the claims made in the paper.
- The abstract and/or introduction should clearly state the claims made, including the contributions made in the paper and important assumptions and limitations. A No or NA answer to this question will not be perceived well by the reviewers.
- The claims made should match theoretical and experimental results, and reflect how much the results can be expected to generalize to other settings.
- It is fine to include aspirational goals as motivation as long as it is clear that these goals are not attained by the paper.

### 2. Limitations

Question: Does the paper discuss the limitations of the work performed by the authors?

Answer: [\[Yes\]](#)

Justification: We have discussed the limitations of the work in the conclusion section.

Guidelines:

- The answer NA means that the paper has no limitation while the answer No means that the paper has limitations, but those are not discussed in the paper.
- The authors are encouraged to create a separate "Limitations" section in their paper.
- The paper should point out any strong assumptions and how robust the results are to violations of these assumptions (e.g., independence assumptions, noiseless settings, model well-specification, asymptotic approximations only holding locally). The authors should reflect on how these assumptions might be violated in practice and what the implications would be.
- The authors should reflect on the scope of the claims made, e.g., if the approach was only tested on a few datasets or with a few runs. In general, empirical results often depend on implicit assumptions, which should be articulated.
- The authors should reflect on the factors that influence the performance of the approach. For example, a facial recognition algorithm may perform poorly when image resolution is low or images are taken in low lighting. Or a speech-to-text system might not be used reliably to provide closed captions for online lectures because it fails to handle technical jargon.
- The authors should discuss the computational efficiency of the proposed algorithms and how they scale with dataset size.
- If applicable, the authors should discuss possible limitations of their approach to address problems of privacy and fairness.
- While the authors might fear that complete honesty about limitations might be used by reviewers as grounds for rejection, a worse outcome might be that reviewers discover limitations that aren't acknowledged in the paper. The authors should use their best judgment and recognize that individual actions in favor of transparency play an important role in developing norms that preserve the integrity of the community. Reviewers will be specifically instructed to not penalize honesty concerning limitations.

### 3. Theory assumptions and proofs

Question: For each theoretical result, does the paper provide the full set of assumptions and a complete (and correct) proof?

Answer: [\[Yes\]](#)

Justification: All theoretical results are accompanied by their full assumptions and complete proofs.

Guidelines:

- The answer NA means that the paper does not include theoretical results.
- All the theorems, formulas, and proofs in the paper should be numbered and cross-referenced.
- All assumptions should be clearly stated or referenced in the statement of any theorems.
- The proofs can either appear in the main paper or the supplemental material, but if they appear in the supplemental material, the authors are encouraged to provide a short proof sketch to provide intuition.
- Inversely, any informal proof provided in the core of the paper should be complemented by formal proofs provided in appendix or supplemental material.
- Theorems and Lemmas that the proof relies upon should be properly referenced.

#### 4. Experimental result reproducibility

Question: Does the paper fully disclose all the information needed to reproduce the main experimental results of the paper to the extent that it affects the main claims and/or conclusions of the paper (regardless of whether the code and data are provided or not)?

Answer: **[Yes]**

Justification: All key implementation and configuration details are provided to ensure reproducibility of the main results.

Guidelines:

- The answer NA means that the paper does not include experiments.
- If the paper includes experiments, a No answer to this question will not be perceived well by the reviewers: Making the paper reproducible is important, regardless of whether the code and data are provided or not.
- If the contribution is a dataset and/or model, the authors should describe the steps taken to make their results reproducible or verifiable.
- Depending on the contribution, reproducibility can be accomplished in various ways. For example, if the contribution is a novel architecture, describing the architecture fully might suffice, or if the contribution is a specific model and empirical evaluation, it may be necessary to either make it possible for others to replicate the model with the same dataset, or provide access to the model. In general, releasing code and data is often one good way to accomplish this, but reproducibility can also be provided via detailed instructions for how to replicate the results, access to a hosted model (e.g., in the case of a large language model), releasing of a model checkpoint, or other means that are appropriate to the research performed.
- While NeurIPS does not require releasing code, the conference does require all submissions to provide some reasonable avenue for reproducibility, which may depend on the nature of the contribution. For example
  - (a) If the contribution is primarily a new algorithm, the paper should make it clear how to reproduce that algorithm.
  - (b) If the contribution is primarily a new model architecture, the paper should describe the architecture clearly and fully.
  - (c) If the contribution is a new model (e.g., a large language model), then there should either be a way to access this model for reproducing the results or a way to reproduce the model (e.g., with an open-source dataset or instructions for how to construct the dataset).
  - (d) We recognize that reproducibility may be tricky in some cases, in which case authors are welcome to describe the particular way they provide for reproducibility. In the case of closed-source models, it may be that access to the model is limited in some way (e.g., to registered users), but it should be possible for other researchers to have some path to reproducing or verifying the results.

#### 5. Open access to data and code

Question: Does the paper provide open access to the data and code, with sufficient instructions to faithfully reproduce the main experimental results, as described in supplemental material?

Answer: [\[Yes\]](#)

Justification: The code and data are publicly available, with clear instructions for reproducing the main results provided in the supplemental material.

Guidelines:

- The answer NA means that paper does not include experiments requiring code.
- Please see the NeurIPS code and data submission guidelines (<https://nips.cc/public/guides/CodeSubmissionPolicy>) for more details.
- While we encourage the release of code and data, we understand that this might not be possible, so “No” is an acceptable answer. Papers cannot be rejected simply for not including code, unless this is central to the contribution (e.g., for a new open-source benchmark).
- The instructions should contain the exact command and environment needed to run to reproduce the results. See the NeurIPS code and data submission guidelines (<https://nips.cc/public/guides/CodeSubmissionPolicy>) for more details.
- The authors should provide instructions on data access and preparation, including how to access the raw data, preprocessed data, intermediate data, and generated data, etc.
- The authors should provide scripts to reproduce all experimental results for the new proposed method and baselines. If only a subset of experiments are reproducible, they should state which ones are omitted from the script and why.
- At submission time, to preserve anonymity, the authors should release anonymized versions (if applicable).
- Providing as much information as possible in supplemental material (appended to the paper) is recommended, but including URLs to data and code is permitted.

## 6. Experimental setting/details

Question: Does the paper specify all the training and test details (e.g., data splits, hyper-parameters, how they were chosen, type of optimizer, etc.) necessary to understand the results?

Answer: [\[Yes\]](#)

Justification: All relevant training and evaluation details are clearly specified in the paper.

Guidelines:

- The answer NA means that the paper does not include experiments.
- The experimental setting should be presented in the core of the paper to a level of detail that is necessary to appreciate the results and make sense of them.
- The full details can be provided either with the code, in appendix, or as supplemental material.

## 7. Experiment statistical significance

Question: Does the paper report error bars suitably and correctly defined or other appropriate information about the statistical significance of the experiments?

Answer: [\[No\]](#)

Justification: Error bars are omitted because the observed variance was minimal and had no impact on the conclusions.

Guidelines:

- The answer NA means that the paper does not include experiments.
- The authors should answer “Yes” if the results are accompanied by error bars, confidence intervals, or statistical significance tests, at least for the experiments that support the main claims of the paper.
- The factors of variability that the error bars are capturing should be clearly stated (for example, train/test split, initialization, random drawing of some parameter, or overall run with given experimental conditions).

- The method for calculating the error bars should be explained (closed form formula, call to a library function, bootstrap, etc.)
- The assumptions made should be given (e.g., Normally distributed errors).
- It should be clear whether the error bar is the standard deviation or the standard error of the mean.
- It is OK to report 1-sigma error bars, but one should state it. The authors should preferably report a 2-sigma error bar than state that they have a 96% CI, if the hypothesis of Normality of errors is not verified.
- For asymmetric distributions, the authors should be careful not to show in tables or figures symmetric error bars that would yield results that are out of range (e.g. negative error rates).
- If error bars are reported in tables or plots, The authors should explain in the text how they were calculated and reference the corresponding figures or tables in the text.

## 8. Experiments compute resources

Question: For each experiment, does the paper provide sufficient information on the computer resources (type of compute workers, memory, time of execution) needed to reproduce the experiments?

Answer: **[Yes]**

Justification: The type of hardware and execution time are specified for all experiments in the paper.

Guidelines:

- The answer NA means that the paper does not include experiments.
- The paper should indicate the type of compute workers CPU or GPU, internal cluster, or cloud provider, including relevant memory and storage.
- The paper should provide the amount of compute required for each of the individual experimental runs as well as estimate the total compute.
- The paper should disclose whether the full research project required more compute than the experiments reported in the paper (e.g., preliminary or failed experiments that didn't make it into the paper).

## 9. Code of ethics

Question: Does the research conducted in the paper conform, in every respect, with the NeurIPS Code of Ethics <https://neurips.cc/public/EthicsGuidelines>?

Answer: **[Yes]**

Justification: The research adheres to the NeurIPS Code of Ethics and does not raise ethical concerns.

Guidelines:

- The answer NA means that the authors have not reviewed the NeurIPS Code of Ethics.
- If the authors answer No, they should explain the special circumstances that require a deviation from the Code of Ethics.
- The authors should make sure to preserve anonymity (e.g., if there is a special consideration due to laws or regulations in their jurisdiction).

## 10. Broader impacts

Question: Does the paper discuss both potential positive societal impacts and negative societal impacts of the work performed?

Answer: **[NA]**

Justification: The paper addresses low-level efficiency improvements for LLM inference and is not directly tied to applications with societal impact.

Guidelines:

- The answer NA means that there is no societal impact of the work performed.
- If the authors answer NA or No, they should explain why their work has no societal impact or why the paper does not address societal impact.

- Examples of negative societal impacts include potential malicious or unintended uses (e.g., disinformation, generating fake profiles, surveillance), fairness considerations (e.g., deployment of technologies that could make decisions that unfairly impact specific groups), privacy considerations, and security considerations.
- The conference expects that many papers will be foundational research and not tied to particular applications, let alone deployments. However, if there is a direct path to any negative applications, the authors should point it out. For example, it is legitimate to point out that an improvement in the quality of generative models could be used to generate deepfakes for disinformation. On the other hand, it is not needed to point out that a generic algorithm for optimizing neural networks could enable people to train models that generate Deepfakes faster.
- The authors should consider possible harms that could arise when the technology is being used as intended and functioning correctly, harms that could arise when the technology is being used as intended but gives incorrect results, and harms following from (intentional or unintentional) misuse of the technology.
- If there are negative societal impacts, the authors could also discuss possible mitigation strategies (e.g., gated release of models, providing defenses in addition to attacks, mechanisms for monitoring misuse, mechanisms to monitor how a system learns from feedback over time, improving the efficiency and accessibility of ML).

## 11. Safeguards

Question: Does the paper describe safeguards that have been put in place for responsible release of data or models that have a high risk for misuse (e.g., pretrained language models, image generators, or scraped datasets)?

Answer: [NA]

Justification: The paper presents infrastructure-level optimizations without releasing any high-risk models or datasets.

Guidelines:

- The answer NA means that the paper poses no such risks.
- Released models that have a high risk for misuse or dual-use should be released with necessary safeguards to allow for controlled use of the model, for example by requiring that users adhere to usage guidelines or restrictions to access the model or implementing safety filters.
- Datasets that have been scraped from the Internet could pose safety risks. The authors should describe how they avoided releasing unsafe images.
- We recognize that providing effective safeguards is challenging, and many papers do not require this, but we encourage authors to take this into account and make a best faith effort.

## 12. Licenses for existing assets

Question: Are the creators or original owners of assets (e.g., code, data, models), used in the paper, properly credited and are the license and terms of use explicitly mentioned and properly respected?

Answer: [Yes]

Justification: We cite all external code and datasets used in the paper, and ensure their licenses and usage terms are properly followed.

Guidelines:

- The answer NA means that the paper does not use existing assets.
- The authors should cite the original paper that produced the code package or dataset.
- The authors should state which version of the asset is used and, if possible, include a URL.
- The name of the license (e.g., CC-BY 4.0) should be included for each asset.
- For scraped data from a particular source (e.g., website), the copyright and terms of service of that source should be provided.

- If assets are released, the license, copyright information, and terms of use in the package should be provided. For popular datasets, [paperswithcode.com/datasets](https://paperswithcode.com/datasets) has curated licenses for some datasets. Their licensing guide can help determine the license of a dataset.
- For existing datasets that are re-packaged, both the original license and the license of the derived asset (if it has changed) should be provided.
- If this information is not available online, the authors are encouraged to reach out to the asset's creators.

### 13. New assets

Question: Are new assets introduced in the paper well documented and is the documentation provided alongside the assets?

Answer: [Yes]

Justification: The new code introduced in the paper is publicly released with clear documentation and usage instructions.

Guidelines:

- The answer NA means that the paper does not release new assets.
- Researchers should communicate the details of the dataset/code/model as part of their submissions via structured templates. This includes details about training, license, limitations, etc.
- The paper should discuss whether and how consent was obtained from people whose asset is used.
- At submission time, remember to anonymize your assets (if applicable). You can either create an anonymized URL or include an anonymized zip file.

### 14. Crowdsourcing and research with human subjects

Question: For crowdsourcing experiments and research with human subjects, does the paper include the full text of instructions given to participants and screenshots, if applicable, as well as details about compensation (if any)?

Answer: [NA]

Justification: No human subjects or crowdsourcing were involved in this study.

Guidelines:

- The answer NA means that the paper does not involve crowdsourcing nor research with human subjects.
- Including this information in the supplemental material is fine, but if the main contribution of the paper involves human subjects, then as much detail as possible should be included in the main paper.
- According to the NeurIPS Code of Ethics, workers involved in data collection, curation, or other labor should be paid at least the minimum wage in the country of the data collector.

### 15. Institutional review board (IRB) approvals or equivalent for research with human subjects

Question: Does the paper describe potential risks incurred by study participants, whether such risks were disclosed to the subjects, and whether Institutional Review Board (IRB) approvals (or an equivalent approval/review based on the requirements of your country or institution) were obtained?

Answer: [NA]

Justification: No human subjects were involved in this study.

Guidelines:

- The answer NA means that the paper does not involve crowdsourcing nor research with human subjects.
- Depending on the country in which research is conducted, IRB approval (or equivalent) may be required for any human subjects research. If you obtained IRB approval, you should clearly state this in the paper.

- We recognize that the procedures for this may vary significantly between institutions and locations, and we expect authors to adhere to the NeurIPS Code of Ethics and the guidelines for their institution.
- For initial submissions, do not include any information that would break anonymity (if applicable), such as the institution conducting the review.

## 16. Declaration of LLM usage

Question: Does the paper describe the usage of LLMs if it is an important, original, or non-standard component of the core methods in this research? Note that if the LLM is used only for writing, editing, or formatting purposes and does not impact the core methodology, scientific rigorousness, or originality of the research, declaration is not required.

Answer: [NA]

Justification: This work does not involve LLMs in the core methodology or contributions.

Guidelines:

- The answer NA means that the core method development in this research does not involve LLMs as any important, original, or non-standard components.
- Please refer to our LLM policy (<https://neurips.cc/Conferences/2025/LLM>) for what should or should not be described.

## A Appendix

### A.1 Psumbook Build vs. Read Breakdown

We quantify the relative cost of constructing and consuming the *Psumbook* by isolating execution to a single SM and splitting runtime into two phases: building the Psumbook for each tile and reading it during the main accumulate loop. We sweep tile width  $t_w$  and batch size  $M$  while fixing  $(N, K)$  as indicated, and we report the *percentage of execution cycles* devoted to each phase for two kernel variants, m2v8 and m1v4.

Across settings, the build/read split is stable with respect to  $M$  at a fixed  $t_w$ , which indicates that Psumbook construction amortizes across the batch. At a fixed  $M$ , larger  $t_w$  increases the build share for small matrices and decreases it for large matrices. Typical ranges are  $\sim 28\text{--}46\%$  build and  $\sim 54\text{--}72\%$  read for m2v8, and  $\sim 20\text{--}42\%$  build and  $\sim 58\text{--}80\%$  read for m1v4.

Table 6: Cycle share (%) spent on building vs. reading the Psumbook under varying  $t_w$  and  $M$ .

$M$	$N$	$K$	$t_w$	Psumbook Phase (%)	Proposed_m2v8	Proposed_m1v4
1	4096	4096	32	Building / Reading	30.5 / 69.5	20.3 / 79.7
1	4096	4096	64	Building / Reading	33.0 / 67.0	28.5 / 71.5
1	4096	4096	128	Building / Reading	31.2 / 68.8	30.7 / 69.3
1	8192	8192	32	Building / Reading	45.4 / 54.6	41.2 / 58.8
1	8192	8192	64	Building / Reading	45.6 / 54.4	39.7 / 60.3
1	8192	8192	128	Building / Reading	28.3 / 71.7	29.5 / 70.5
4	4096	4096	32	Building / Reading	30.4 / 69.6	20.7 / 79.3
8	4096	4096	32	Building / Reading	30.7 / 69.3	20.4 / 79.6
4	8192	8192	32	Building / Reading	45.7 / 54.3	41.3 / 58.7
8	8192	8192	32	Building / Reading	46.1 / 53.9	41.6 / 58.4

### A.2 Tile Size Sensitivity

We revisited our heuristic choices for the tile dimensions and conducted a systematic sweep over  $t_w \in \{32, 64, 128\}$  and  $t_h \in \{2048, 4096\}$  across representative shapes. We find that  $t_h=2048$  consistently yields the best performance over a broad set of workloads, supporting our original choice. For the horizontal tile, smaller values such as  $t_w=32$  work well for relatively small matrices, whereas  $t_w=64$  tends to perform better on large matrices. We attribute this to coarser tiling reducing kernel-launch overhead and improving partial-sum reduction efficiency at scale. Table 7 summarizes representative

results for  $(N, K) \in \{(4096, 4096), (8192, 8192)\}$  at  $M=1$ . Overall, these observations justify our default choice  $(t_w, t_h) = (32, 2048)$  for small and medium shapes, with  $t_w=64$  preferred as matrices grow.

Table 7: Effect of tile dimensions on end-to-end latency ( $\mu$ s).

$M$	$N$	$K$	$t_w$	$t_h$	Proposed_m2v8	Proposed_m1v4
1	4096	4096	32	2048	26.57	25.07
1	4096	4096	64	2048	26.76	25.40
1	4096	4096	128	2048	29.61	26.81
1	4096	4096	32	4096	28.95	27.60
1	4096	4096	64	4096	28.49	27.68
1	4096	4096	128	4096	37.58	32.87
1	8192	8192	32	2048	39.04	36.02
1	8192	8192	64	2048	37.23	35.33
1	8192	8192	128	2048	40.09	38.54
1	8192	8192	32	4096	37.78	36.17
1	8192	8192	64	4096	38.29	37.70
1	8192	8192	128	4096	45.40	42.75

### A.3 Effect of Higher Bit Precision

We additionally measured latency for higher average bit precisions using the kernel configuration ( $g=128$ ,  $b=8$ ,  $t_w=32$ ,  $t_h=2048$ ). For reference, FP16 cuBLAS latency is included. As expected, increasing the effective bits per weight (via larger numbers of codebooks  $m$  or smaller vector length  $v$ ) generally raises latency, and the trend is more pronounced for larger matrices (e.g.,  $M=1$ ,  $N=K=8192$ ). Even at higher bit precisions, *CodeGEMM* remains competitive with FP16 baselines while offering a flexible accuracy–efficiency trade-off through the  $(m, v)$  configuration.

Table 8: Matrix multiplication latency ( $\mu$ s) for higher effective bit precisions under ( $g=128$ ,  $b=8$ ,  $t_w=32$ ,  $t_h=2048$ ). FP16 cuBLAS is shown for reference.

$M$	$N$	$K$	$m$	$v$	bit	latency
1	4096	4096	N/A	N/A	16.000	28.118
1	4096	4096	1	4	2.126	25.074
1	4096	4096	2	4	4.127	27.009
1	4096	4096	1	8	1.127	24.015
1	4096	4096	2	8	2.129	26.574
1	4096	4096	3	8	3.126	27.385
1	4096	4096	4	8	4.127	29.797
1	8192	8192	N/A	N/A	16.000	95.785
1	8192	8192	1	4	2.125	36.020
1	8192	8192	2	4	4.125	49.636
1	8192	8192	1	8	1.125	31.883
1	8192	8192	2	8	2.126	39.040
1	8192	8192	3	8	3.126	47.210
1	8192	8192	4	8	4.127	58.364

### A.4 Batch-Size Sensitivity and Fair cuBLAS Accounting

For fair comparison, we include the dequantization stage when reporting FP16 cuBLAS latency, since dequantization is required to precede GEMM in codebook-based pipelines. Under this accounting, *CodeGEMM* remains competitive even at batch sizes of 8 and 16. In data-center deployments, continuous batching can aggregate requests and increase the effective batch size during decoding; yet, many scenarios still operate with small batches (e.g., on-device inference). The batch-size sensitivity observed in CUDA–core quantized kernels reflects architectural constraints such as occupancy limits and shared-memory bandwidth. This limitation is shared by recent methods (e.g., QuIP# and QTIP) and does not indicate algorithmic inefficiency. Table 9 reports linear latency on Llama-3-8B.

Table 9: Aggregate latency of linear layers ( $\mu s$ ) within a Llama-3-8B decoder block as a function of batch size.

BS	cuBLAS	Dequant	cuBLAS +Dequant	AQLM (1x16)	AQLM (2x8)	QUIP# (e8p)	QTIP (r2)	Proposed (m2v8)	Proposed (m1v4)
1	332	1027	1360	646	250	163	190	172	153
4	333	1027	1361	2373	794	445	550	491	405
8	336	1027	1364	4695	1515	818	1034	909	744
16	340	1027	1367	9267	2959	1554	1991	1748	1416

## A.5 Additional Benchmarks Across Problem Sizes

We expanded our evaluation to a broad sweep of matrix shapes  $(M, N, K)$ . Latency is measured end to end on a fixed hardware and software stack, with all kernels compiled under identical toolchains. Table 10 reports the full results. cuBLAS runs on Tensor Cores and tends to maintain relatively stable latency as the batch size  $M$  grows, whereas recently proposed quantized kernels—including ours—execute on CUDA cores and often show increased latency with larger  $M$ . Within this CUDA-core class, *CodeGEMM* consistently performs well on large matrices, where arithmetic intensity and memory reuse are high. In practice, the method remains competitive across diverse  $(M, N, K)$  settings and is particularly effective for large-scale matrix multiplications that dominate LLM inference.

Table 10: Kernel latency ( $\mu s$ ) across diverse  $(M, N, K)$  configurations.

M	N	K	cuBLAS	AQLM (1x16)	AQLM (2x8)	Proposed (m2v8)	Proposed (m1v4)	QUIP# (e8p)	QTIP (r2)
1	2048	2048	19.82	28.84	20.55	20.75	20.66	19.47	19.44
4	2048	2048	19.99	74.67	43.31	44.04	41.92	36.71	36.00
8	2048	2048	19.79	135.36	73.03	75.18	69.72	59.44	57.87
1	8192	2048	30.57	28.84	28.83	25.94	26.70	25.52	27.08
4	8192	2048	31.31	74.67	76.15	63.97	65.36	60.70	66.18
8	8192	2048	31.70	135.36	138.09	115.39	116.11	107.85	118.99
1	2048	8192	27.52	60.47	30.93	24.28	23.81	23.44	24.90
4	2048	8192	29.82	203.86	82.18	56.21	52.57	51.91	59.03
8	2048	8192	28.69	396.44	149.98	98.92	90.73	89.91	103.24
1	4096	4096	28.00	63.13	32.28	24.76	24.97	23.96	26.74
4	4096	4096	28.54	210.03	89.76	60.58	57.79	53.92	62.74
8	4096	4096	28.11	396.37	165.49	108.16	103.92	93.43	110.84
1	14336	4096	88.67	168.12	64.76	38.85	37.51	38.91	51.30
4	14336	4096	89.08	632.69	217.68	111.20	106.90	113.28	161.23
8	14336	4096	89.29	1252.55	422.89	211.37	196.68	212.55	308.37
1	4096	14336	86.31	169.31	58.70	36.15	33.92	37.27	43.85
4	4096	14336	86.51	635.74	193.41	103.15	92.61	106.63	133.36
8	4096	14336	86.49	1253.11	372.97	192.63	170.16	199.31	252.12
1	8192	8192	96.40	188.91	62.50	37.99	35.45	38.31	49.86
4	8192	8192	100.41	713.24	208.11	111.00	98.66	111.08	157.26
8	8192	8192	95.45	1408.68	402.29	207.73	184.25	208.29	299.24
1	28672	8192	297.74	625.53	181.54	86.48	76.71	101.98	134.03
4	28672	8192	303.10	2462.88	684.92	305.47	264.31	366.74	492.14
8	28672	8192	295.11	4913.52	1355.70	597.22	514.85	718.13	970.35
1	8192	28672	302.42	618.61	180.38	86.20	76.50	101.13	124.90
4	8192	28672	292.59	2437.82	679.24	305.14	263.70	361.95	455.84
8	8192	28672	293.69	4860.85	1344.49	596.63	515.12	710.94	897.41